

Absence of Ion-Binding Affinity in the Putatively Inactivated Low-[K⁺] Structure of the KcsA Potassium Channel

Céline Boiteux¹ and Simon Bernèche^{1,*}

¹Swiss Institute of Bioinformatics, Computational & Systems Biology, Biozentrum, University of Basel, Klingelbergstrasse 50/70, CH-4056 Basel, Switzerland

*Correspondence: simon.berneche@unibas.ch

DOI 10.1016/j.str.2010.10.008

SUMMARY

Potassium channels are membrane proteins that selectively conduct K⁺ across cellular membranes. The narrowest part of their pore, the selectivity filter, is responsible for distinguishing K⁺ from Na⁺, and can also act as a gate through a mechanism known as C-type inactivation. It has been proposed that a conformation of the KcsA channel obtained by crystallization in presence of low concentration of K⁺ (PDB 1K4D) could correspond to the C-type inactivated state. Here, we show using molecular mechanics simulations that such conformation has little ion-binding affinity and that ions do not contribute to its stability. The simulations suggest that, in this conformation, the selectivity filter is mostly occupied by water molecules. Whether such ion-free state of the KcsA channel is physiologically accessible and representative of the inactivated state of eukaryotic channels remains unclear.

INTRODUCTION

Potassium channels regulate ion diffusion across cellular membranes by using different gating mechanisms to vary their conductance. A significant number of experiments support the idea that the selectivity filter, the only region of the pore interacting directly with permeating ions, not only allows the channel to distinguish between K⁺ and Na⁺ but also plays a central role in gating. Gating events in the selectivity filter take place on different timescales, from nanoseconds to seconds. Long-lasting nonconducting states can potentially be associated with C-type (slow) inactivation, which consists in the time-dependent closure of the selectivity filter following the activation of the channel (Yellen, 1998). This inactivation process plays a critical role in controlling the length and frequency of cardiac action potentials, as well as the firing patterns in neurons (Smith et al., 1996; Bean, 2007). C-type inactivation is well known to depend on ion occupancy and permeation (Yellen, 1998), though the molecular details underlying this interdependency of mechanisms are still not clearly understood.

It was proposed that the prokaryotic KcsA potassium channel was subject to C-type inactivation like many eukaryotic voltage-dependent K⁺ channels (Gao et al., 2005; Cordero-Morales et al., 2006). Because the C-type inactivation properties of KcsA are similar to those of its eukaryotic counterparts, notably its sensitivity to external K⁺ concentration (Chakrapani et al., 2007), KcsA seems to be an ideal candidate for structural studies of this inactivation mechanism. Some elements of information on the structural properties of its inactivated state have recently been provided by different experimental techniques and molecular mechanics simulations (Zhou et al., 2001; Bernèche and Roux, 2005; Lenaeus et al., 2005; Cordero-Morales et al., 2006, 2007; Domene et al., 2008; Ader et al., 2008). Crystals of the KcsA channel that were grown in the presence of extremely low concentration of K⁺ (3 mM) have revealed an alternative conformation of the selectivity filter that appears to be nonconducting (PDB entry 1K4D) (Zhou et al., 2001). This “low-[K⁺]” structure was proposed by MacKinnon and coworkers (Zhou et al., 2001) as a key state in the physiological regulation of the conductance of K⁺ channels. Other authors have proposed that this nonconducting conformation of the KcsA channel could correspond to a C-type inactivated state of the channel (Yellen, 2001; Cordero-Morales et al., 2007; Ader et al., 2008). Although the structural analysis of this static conformation suggests that pore lining amide hydrogen atoms would prevent the permeation of ions, uncertainties remain about its ion occupancy state and stability under physiological conditions. It is notably unclear, considering the high concentration of sodium salt used in the crystallization experiment, whether K⁺ or Na⁺ should be expected in the selectivity filter. To address these questions, we performed explicit molecular dynamics simulations of the KcsA channel in its nonconducting low-[K⁺] conformation, comparing different occupancy states involving both K⁺ and Na⁺. As a control, we also performed simulations based on the canonical, high-[K⁺] structure (PDB entry 1K4C) (Zhou et al., 2001). Combined with free-energy calculations, these simulations show that ions are unexpectedly unstable in the low-[K⁺] conformation of the selectivity filter and that their replacement by water molecules has no impact on the structure of the channel. It remains unclear if the low-[K⁺] conformation, without any ion bound to the filter, is visited under normal conditions of conduction and inactivation.

RESULTS

Absence of Ion-Binding Affinity

We started by performing simulations of the low-[K⁺] structure embedded in a membrane bilayer with different initial ion occupancy states (Table 1). Simulations with one or two ions bound to the selectivity filter show essentially the same behaviors (Figures 1 and 2; see Figures S1 and S2 available online). In all of these simulations, K⁺ and Na⁺ left the channel within a few nanoseconds of simulation. All efforts to further stabilize the ions have been in vain. The structure of the protein is not affected in any way by the departure of ions, which are replaced by water molecules. The conformation of the selectivity filter remains stable within the normal thermal fluctuations. As reference, similar simulations based on the canonical KcsA structure show stable trajectories with ions remaining bound to the selectivity filter, though some brief excursions of an ion from binding site S4 to the cavity are occasionally observed (Figure S3). The trajectory presented in Figure 1A shows that K⁺ finds two metastable positions in the lower part of the selectivity filter, around binding site S4. The calculation of electronic density along the channel's pore reveals that water molecules occupy positions that exactly match the density peaks obtained by X-ray diffraction (Figures 1B and 1C). The elongated peak of electronic density observed around binding site S4 could correspond to the juxtaposition of an ion and a water molecule in two alternating configurations. Figure 2 presents simulations in which one of the S1 or S4 binding sites is initially occupied by Na⁺. The trajectories illustrate that Na⁺ is not stable in S1 and that it binds less frequently to the upper-S4 binding site than K⁺. The lower-S4 binding site is alternately occupied by K⁺ and Na⁺ and, thus, does not seem to be selective.

To more precisely describe the interaction between ions and the selectivity filter, we calculated radial distribution functions, $g(r)$, describing the ion coordination shells, which are composed of oxygen atoms from water molecules and protein chemical groups (backbone carbonyl and hydroxyl of Thr75). The radial distribution functions plotted in Figure 3A and the associated coordination number functions, $n(r)$, in Figure 3C illustrate that the S1-binding site in the low-[K⁺] conformation does not properly coordinate K⁺. The canonical high-[K⁺] structure shows quite strong K⁺ coordination with eight ligands found within 3.5 Å (the approximate distance of the first minima in the $g(r)$ presented in Figure 3A), whereas the corresponding number of ligands in the low-[K⁺] conformation is below the reference bulk value of about six ligands. Actually, in the latter conformation the protein provides only four coordinating ligands, as indicated by the dashed line in Figure 3C. The low-[K⁺] structure provides better coordination in S4 than in S1, but the number of ligands remains lower than in the high-[K⁺] structure (Figures 3B and 3D). Like in S1, the first coordination shell in S4 includes more water molecules in the low-[K⁺] conformation than in the high-[K⁺] one, which is likely to increase the impact of thermal fluctuations on the stability of the ion. When bound to the lower S4-binding site, K⁺ is coordinated by only four or five protein ligands. The coordination of Na⁺ in S1 and S4 is nearly equivalent to that of K⁺, with the exception that Na⁺ does not bind to the upper-S4 binding site. Figure 4 shows that when Na⁺ is in the lower S4

Table 1. Initial Ion Occupancy State of the Different Simulations

Simulation label	S ₀	S ₁	S ₂	S ₃	S ₄	Cav	Duration
High-[K ⁺] (PDB 1k4c)							
HK ₁ K ₃ K	W	K	W	K	W	K	10 ns
HK ₂ K ₄	W	W	K	W	K	W	10 ns
HW	W	W	W	W	W	∅	30 ns
Low-[K ⁺] (PDB 1k4d)							
LK ₁	W	K	∅	W	W	∅	10 ns
LK ₄	W	W	∅	W	K	∅	10 ns
LK ₁ K ₄	W	K	∅	W	K	∅	10 ns
LK ₁ K ₄ Na	W	K	∅	W	K	Na	18 ns
LNa ₁ K ₄ Na	W	Na	∅	W	K	Na	10 ns
LK ₁ Na ₄ Na	W	K	∅	W	Na	Na	10 ns
LNa ₁ K ₄	W	Na	∅	W	K	∅	5 ns
LK ₁ Na ₄	W	K	∅	W	Na	∅	5 ns
LW	W	W	∅	W	W	∅	10 ns

K, potassium; Na, sodium; W, water molecule; ∅, empty.

site, only two or three of its coordinating ligands are provided by the protein.

Although the radial distribution function tells us about the interactions taking place in given binding sites, it does not inform us on the actual binding affinity. To obtain this information we have computed the potential of mean force (PMF) describing the ion displacement along the pore axis around the S1 and S4 binding sites (Figure 5). The calculations show that, when ions are placed in the cavity and S4, the binding site S1 is less stable than bulk water by about 2.8 kcal/mol for K⁺ and 4 kcal/mol for Na⁺ (Figure 5A, solid lines). As a comparison, under similar conditions, a K⁺ in the S1 binding site of the canonical high-[K⁺] structure is retained in a well of about 6 kcal/mol (Bernèche and Roux, 2001). This important free-energy difference of about 9 kcal/mol is attributable to the slight variation of the coordination shell as described above. It is interesting to note that Na⁺ binds a bit deeper at $Z = 3.8$ Å than K⁺, which binds at $Z = 4.5$ Å. As illustrated by the insets of Figure 5A, the smaller radius of Na⁺ allows it to find an equilibrium position almost in the plane of a row of carbonyl groups, whereas the bigger K⁺ requires interactions with two of these rows. K⁺ and Na⁺ are stabilized in wells with depths of 2.9 and 0.9 kcal/mol, respectively. If ions are removed from the cavity and S4, thereby reducing the ion-ion repulsion, the S1 binding site in the low-[K⁺] structure becomes more favorable with a free-energy level comparable to the reference bulk value. However, the free-energy wells remain shallow (~2 kcal/mol depth) for both ion types, allowing the ions to diffuse to the bulk within a few nanoseconds of simulations, as illustrated by the time series of Figure S1B. The PMFs presented in Figure 5B show that, in absence of an ion in S1, stable but shallow binding sites are also found in the lower part of S4, with depths of -1.5 kcal/mol ($Z = -7$ Å) and -2.4 kcal/mol ($Z = -6$ Å) for K⁺ and Na⁺, respectively. For K⁺, an extra metastable binding site is seen at $Z = -5$ Å, which corresponds to the upper S4 binding site. The PMFs of Figure 5B depict the configuration illustrated by trajectories of Figures S1 and S2, i.e., without an ion initially bound to the cavity. Adding an ion in the cavity would, by the action of ion-ion repulsion, further

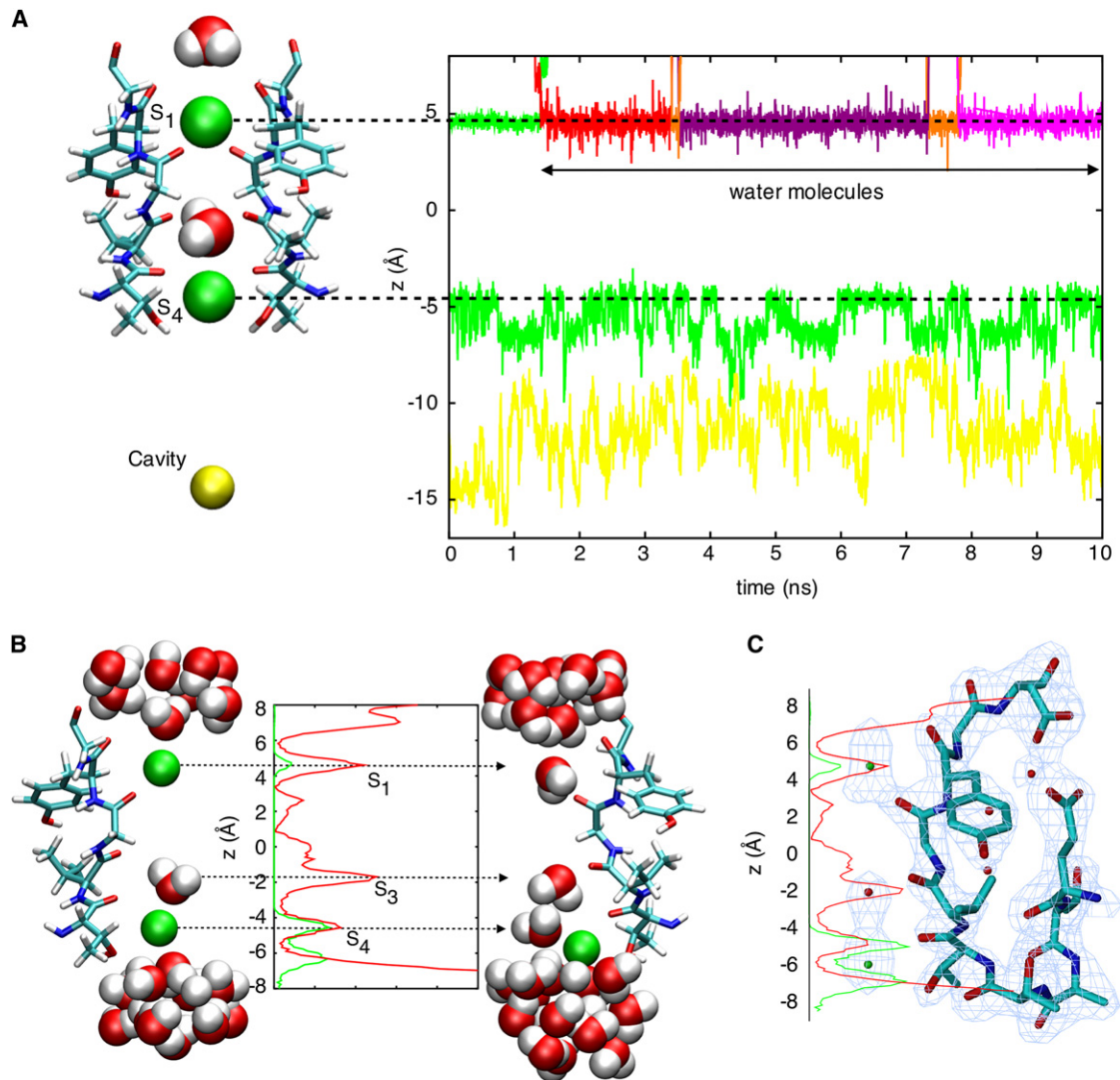


Figure 1. Simulation of the Low-[K⁺] Structure with K⁺ (green spheres) in Binding Sites S1 and S4, and a Na⁺ (yellow sphere) in the Cavity
 (A) The time series analysis shows that the K⁺ in S1 (green line) leaves the selectivity filter after about 250 ps of simulation and is replaced by water molecules (purple, red, and orange lines). The ion in S4 is also not tightly bound, frequently leaving the binding site for excursions of various duration in the cavity.
 (B) The graph presents molecular densities along the pore axis extracted from the simulation described in (A). The red curve corresponds to water molecules and the green one to K⁺ and Na⁺ together. The molecular density around S4 clearly shows two juxtposed ion-binding sites (upper and lower S4). The molecular representation on the left corresponds to the initial state of the simulation; the one on the right corresponds to the conformation after 5 ns of simulation.
 (C) The calculated electron density along the z axis (derived from the molecular density shown in B considering 18e⁻/K⁺, 10e⁻/Na⁺, and 10e⁻/H₂O) is superimposed with the experimental electron density of the low-[K⁺] structure (PDB entry 1K4D) (Zhou et al., 2001). The small red and green spheres represent water molecules and K⁺ as proposed by Zhou et al. (2001). See also Figure S1.

stabilize K⁺ in the upper-S4 binding site, as seen in Figure 1A. The PMF calculations also show important free-energy barriers around Z = ± 3.5 Å, suggesting that the low-[K⁺] conformation of the channel would not conduct ions. Domene and Furini (2009) have reported PMFs that are consistent with the ones presented here, with energy barriers preventing ion conduction and shallow binding sites of 1.0 and 2.5 kcal/mol depths for Na⁺ and K⁺, respectively. However, based on molecular dynamics simulations, they concluded that Na⁺ and K⁺ are stable in S1 and S4, even in doubly occupied states. The reason for

which they observed such ion stability despite shallow binding sites remains unclear.

Water Molecules Occupy the Selectivity Filter

The low ion-binding affinity of the selectivity filter in its low-[K⁺] conformation suggests that the experimental electronic density that was initially assigned to K⁺ could instead reflect the presence of water molecules. To further test this hypothesis, we have performed simulations of the low-[K⁺] KcsA structure without any ion bound to the selectivity filter. As anticipated,

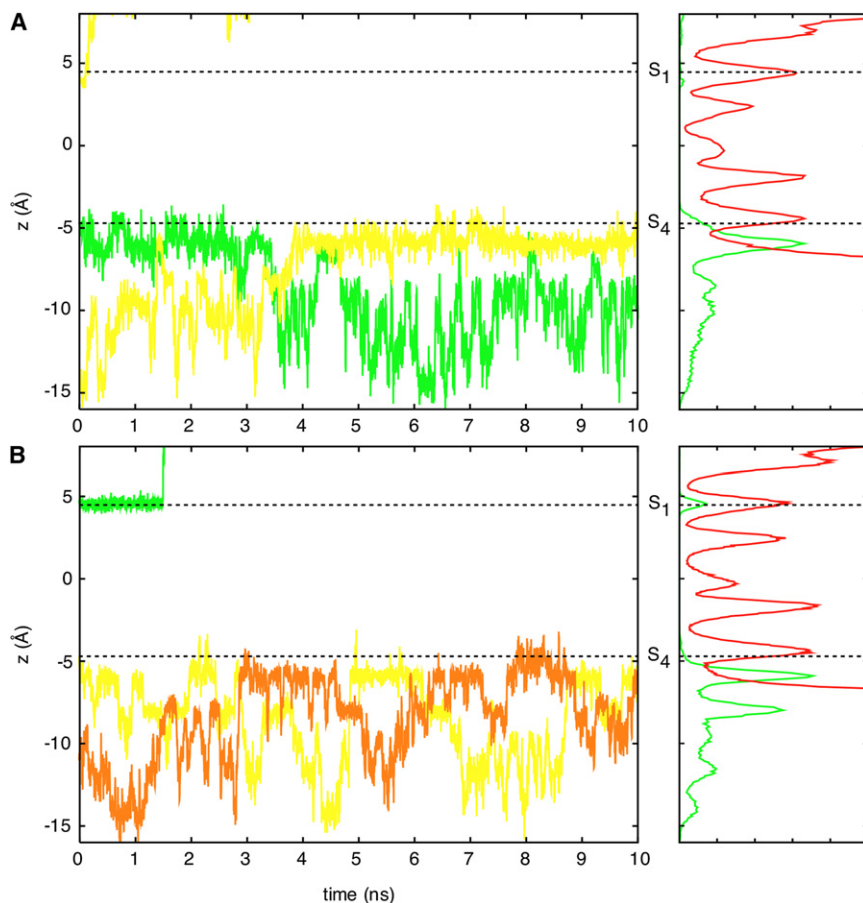


Figure 2. Simulations of the Low-[K⁺] Structure with Na⁺ Alternatively Bound to Sites S1 and S4

The time series describe the position of ions along the simulations LNa₇K₄Na (A) and LK₇Na₄Na (B). The dashed lines indicate the position of the K⁺-binding sites as defined in Figure 1. All K⁺ (green) and Na⁺ (yellow and orange) ions are seen to be rather unstable in both S1 and upper S4. Both Na⁺ and K⁺ bind to lower S4, with some brief excursions to upper S4. The fact that both K⁺ and Na⁺ alternatively bind to lower S4 indicates that the site is not selective. Molecular densities are shown on the right side for water molecules (red) and ions, including both Na⁺ and K⁺ (green). See also Figure S2.

found around the selectivity filter and the hydrogen-bond network that is put in place to stabilize the backbone of the protein (Figures 7B–7G). However, one difference between the two structures is the orientation of the Val76/Gly77 amide plane. Although, overall, the backbones superimpose quite well, these amide planes are flipped by about 180° with their carbonyl groups and nitrogen atoms pointing in opposite directions (see also Figure S6). It implies that the hydrogen-bond networks in which these chemical groups are involved propagate in opposite directions, while still sharing most of their structural features. In both cases the rotation of the Val76/Gly77 amide

plane brings the carbonyl and nitrogen groups in an orientation tangent to the pore axis, allowing both chemical groups to form hydrogen bonds with water molecules found on either side, in between the subunits (Figures 7C and 7F). These water molecules interacting with the amide planes are further stabilized by participating in short chains of three hydrogen-bonded water molecules (Figures 7B and 7E). As illustrated in Figure 6, both conformations of the Val76/Gly77 amide plane are stable over the timescale of the molecular dynamic simulations. However, it is unclear why one of them is preferred in the crystallization experiment and the other one in the simulation starting with the canonical KcsA structure. The network of hydrogen bonds described in Figure 7 greatly reduces the probability of isomerization between the two conformations, and, thus, isomerization is unlikely to be observed on the timescale of the simulations.

based on the different simulations discussed above, the absence of ions had no impact on the structure of the selectivity filter, which remained stable throughout the 10 ns simulation (Figure 6). We repeated the same computer experiment with the canonical KcsA structure (PDB entry 1K4C) (Zhou et al., 2001). In this case, removing ions leaves the carbonyl groups of the selectivity filter facing each other without any countercharge in between. During the simulation, many water molecules from the bulk solvent are seen entering the region surrounding the selectivity filter, while the protein's backbone undergoes conformational changes consisting of slight rotations of all amide planes (except Val76/Gly77, for which rotation is more important; see below). In simulations performed with ions in the selectivity filter, conformational changes are generally limited to one or two subunits (Bernèche and Roux, 2005; Domene et al., 2008). Here, in absence of ions, the four subunits undergo transitions, and the structure remains 4-fold symmetric within thermal fluctuations. In less than a nanosecond, the structure becomes almost perfectly superposable to the experimental low-[K⁺] structure (Figure 7A) and remains stable for the whole simulation of 30 ns with a backbone root-mean-square deviation oscillating between 1.0 and 1.5 Å from the experimental structure (residues 74–80, excluding the Val76 carbonyl group; see also Figure S5). It is remarkable that all the structural features of the low-[K⁺] conformation are retrieved, notably the three water molecules

plane brings the carbonyl and nitrogen groups in an orientation tangent to the pore axis, allowing both chemical groups to form hydrogen bonds with water molecules found on either side, in between the subunits (Figures 7C and 7F). These water molecules interacting with the amide planes are further stabilized by participating in short chains of three hydrogen-bonded water molecules (Figures 7B and 7E). As illustrated in Figure 6, both conformations of the Val76/Gly77 amide plane are stable over the timescale of the molecular dynamic simulations. However, it is unclear why one of them is preferred in the crystallization experiment and the other one in the simulation starting with the canonical KcsA structure. The network of hydrogen bonds described in Figure 7 greatly reduces the probability of isomerization between the two conformations, and, thus, isomerization is unlikely to be observed on the timescale of the simulations.

DISCUSSION

Our results show that the low-[K⁺] structure of the KcsA channel does not properly coordinate ions and, thus, does not present any strong ion-binding sites. The simulations also suggest that the low-[K⁺] conformation of the selectivity filter does not require any ion to be stable. Simulations of the canonical-conducting conformation of KcsA in which all ions had been replaced by water molecules led to a 4-fold symmetric conformation sharing

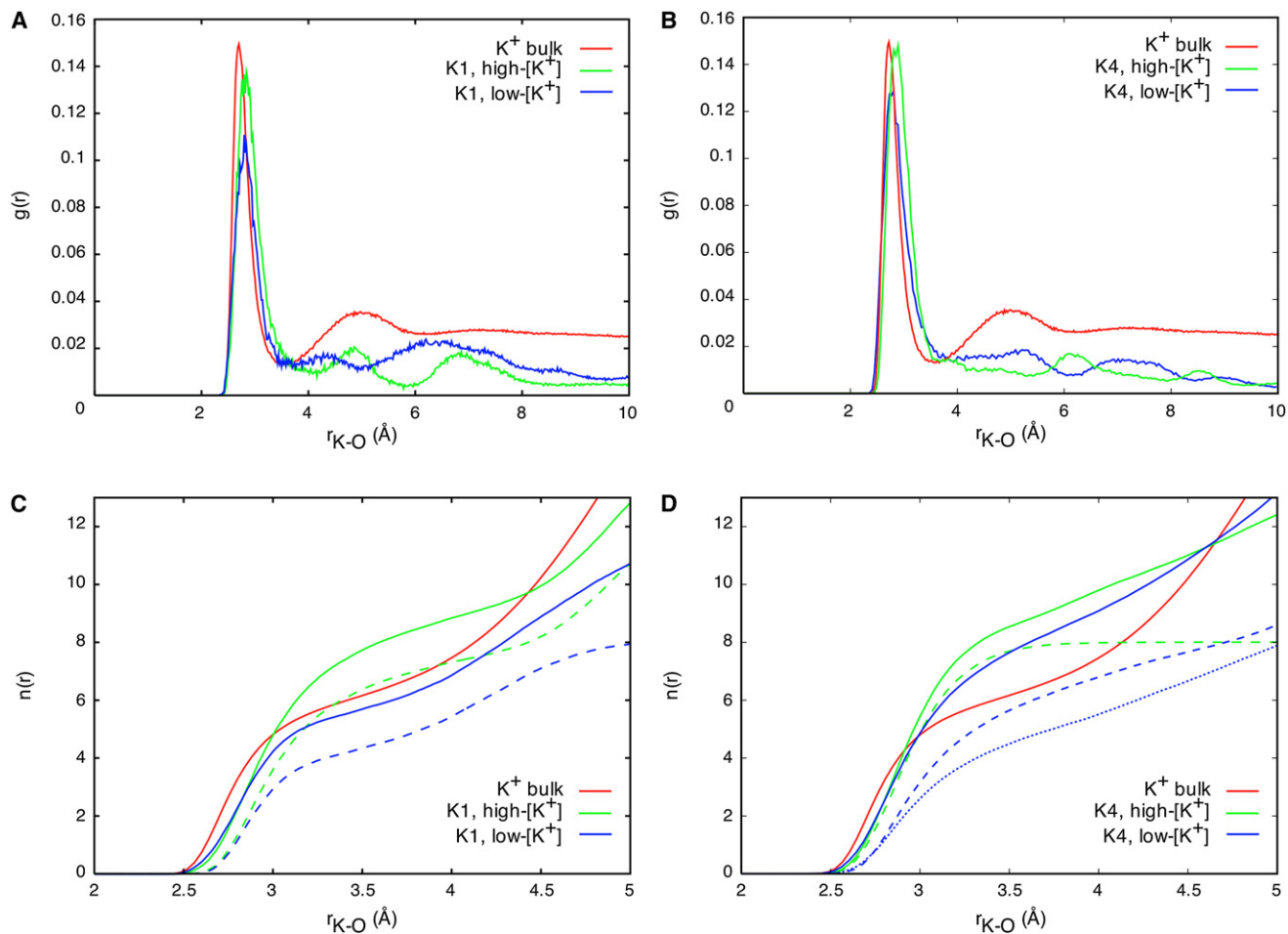


Figure 3. Comparison of the Coordination Shell of K⁺ in Binding Sites S1 and S4 of the Low-[K⁺] and High-[K⁺] Structures

Data for the low-[K⁺] structure are extracted from simulation LK₁K₄Na presented in Figure 1 ($t = 0.2$ – 1.0 ns for S1, and $t = 6.1$ – 6.9 ns for S4). Reference values from the canonical high-[K⁺] structure were calculated based on the simulations of Figure S3.

(A and B) show radial distribution functions, $g(r)$, of oxygen atoms (from water molecules and protein carbonyl and hydroxyl groups) around K⁺. The $g(r)$ in (A) show that an ion bound to S1 in the low-[K⁺] structure is not coordinated as well as in the high-[K⁺] one. However, as suggested by the plot in (B), K⁺ coordination in S4 seems almost equivalent for both structures.

(C and D) plot the distance-dependent coordination number, $n(r)$, including oxygen atoms from water molecules and protein chemical groups (solid line), or only the latter (dashed line). In both S1 and S4, a K⁺ bound to the low-[K⁺] structure has two fewer protein ligands in its first coordination shell ($r < 3.5$ Å) than in the high-[K⁺] structure. When bound to the lower S4-binding site, K⁺ loses one to two more protein ligands (blue dotted line in D). The reduced number of protein ligands explains why a K⁺ in S4 is more loosely bound in the low-[K⁺] than the high-[K⁺] structure.

many features with the low-[K⁺] structure. Such ion-free KcsA simulations have been performed before, but none of these has actually shown a 4-fold symmetric conformation (Furini et al., 2009). However, a 2-fold symmetry involving conformational changes in the selectivity filter was reported for simulation systems with K⁺ present in the selectivity filter (Cordero-Morales et al., 2007; Domene et al., 2008).

In all of our simulations of the low-[K⁺] structure initiated with K⁺ or Na⁺ in the selectivity filter, the S1, S3, and S4 binding sites are mostly occupied by water molecules, whereas S2 remains inaccessible. The lower part of site S4 can be transiently occupied by K⁺ or Na⁺ without preference and with little binding affinity. Only K⁺ can occasionally reach the upper S4 site, provided that another ion occupies the cavity. The electronic densities calculated on the basis of the MD simulations (Figures

1 and 2) are in good agreement with the experimental density obtained by X-ray diffraction (Zhou et al., 2001). When water molecules replace ions in the selectivity filter, the positions of the calculated electronic density peaks remain unchanged. The simulations illustrate that the wide density peak around S4 could well correspond to a water molecule juxtaposed to an ion (Na⁺ or K⁺). The S1 and S4 binding sites present some differences from both a structural and an energetics point of view. However, these differences are not as important as what the density plots of Figures 1 and 2 might suggest. Binding events in S4 are more frequent than in S1, in large part because ions are trapped in the cavity below the selectivity filter and cannot diffuse away because the main gate on the intracellular side of the pore is closed. In this context the apparent concentration of ions near S4 might be much higher than the bulk concentration.

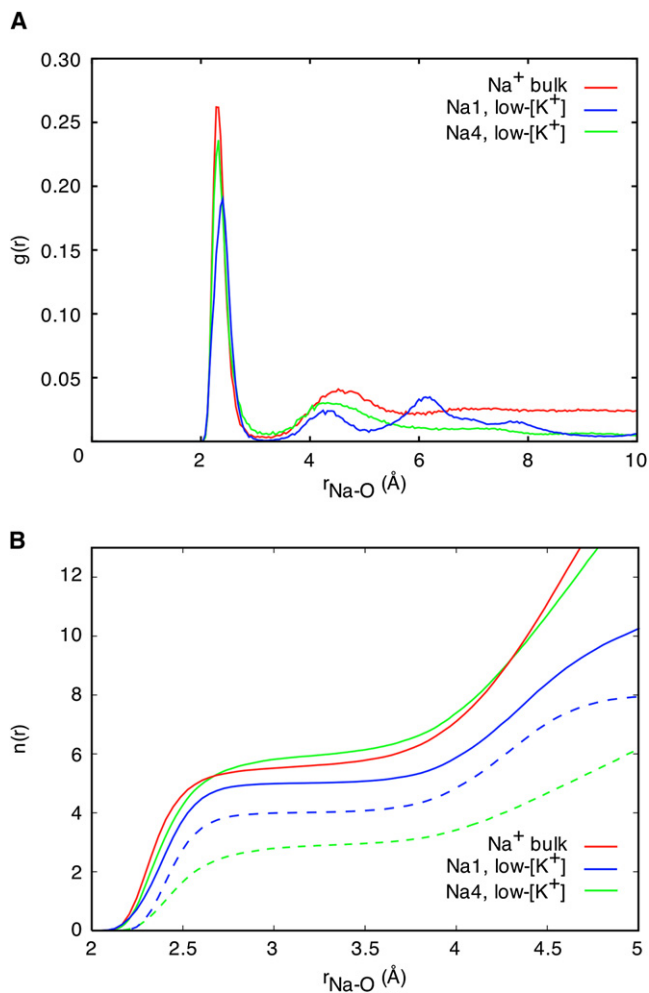


Figure 4. Coordination of Na⁺ in the S1 and S4 Binding Sites of the Low-[K⁺] Structure

Data are taken from simulations LNa₁K₄ for S1 (Figure S3) ($t = 0.2$ – 1.0 ns) and LK₁Na₄Na for S4 (Figure 2, $t = 5.0$ – 5.8 ns). In (A), radial distribution functions of oxygen atoms around Na⁺ show a better coordination in S4 (Na₄) than S1 (Na₁). The deficit of coordinating ligands in S1 explains the instability of Na⁺ in this binding site. In (B) the coordination number functions for Na⁺ in S1 and S4 are shown, including all oxygen atoms (solid line) or only those provided by the protein (dashed line). A Na⁺ in S4 finds a proper coordination shell with about six ligands within 3 Å, but only two of these are provided by the protein itself.

The idea that both S1 and S4 present low ion-binding affinities is supported by an X-ray crystallography titration experiment performed with Tl⁺ (Zhou and MacKinnon, 2003). At low Tl⁺ concentration, the KcsA channel adopts the so-called low-[K⁺] conformation. Interestingly, the titration experiment shows that, at a concentration of 3 mM Tl⁺, there is a total of only 0.1 ion in the selectivity filter, supporting our conclusion that the low-[K⁺] conformation is essentially depleted of ion. Concentrations of 25 and 65 mM Tl⁺ lead to occupancies of ~ 0.5 and ~ 1.0 ion, respectively. For comparison, a $K_d = 25$ mM would correspond approximately to a binding affinity of 2.2 kcal/mol, which is in qualitative agreement with the free-energy wells described by the PMFs of Figure 5. The simulations and the

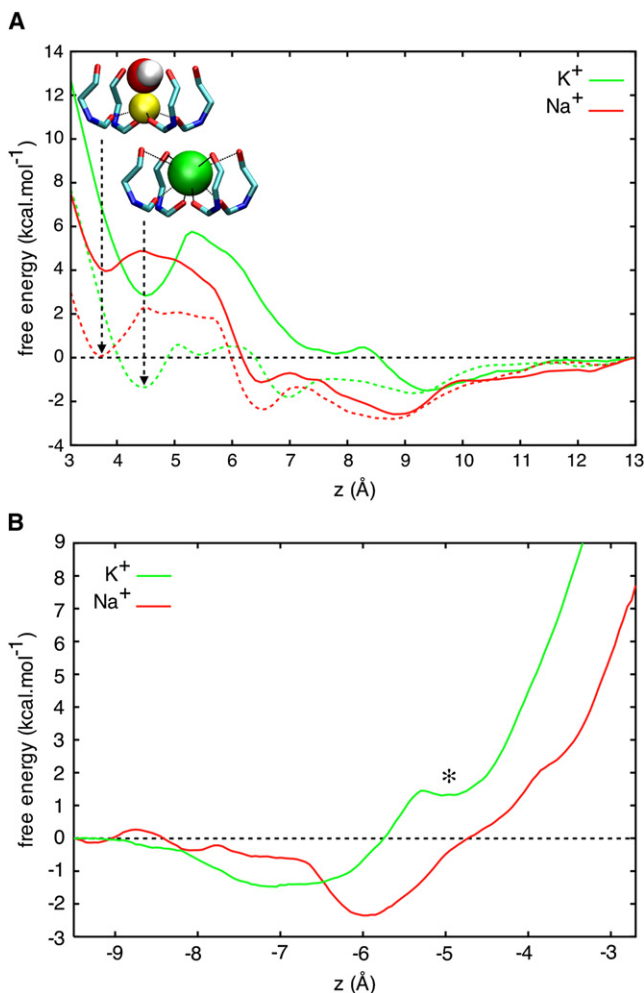


Figure 5. Ion-Binding Affinity of the Low-[K⁺] Structure Described by PMF Calculations Along the Pore Axis

(A) Around binding site S1, K⁺ and Na⁺ have different coordination numbers, their interactions with carbonyl oxygen atoms lead to slightly different equilibrium positions ($Z = 4.5$ Å for K⁺ and $Z = 3.8$ Å for Na⁺), as illustrated by the insets. With ions present in the cavity and S4, the S1-binding site is less stable than bulk water by about 2.8 kcal/mol for K⁺ (solid green line) and 4 kcal/mol for Na⁺ (solid red line). Both ions are stabilized in wells with depths of 2.9 and 0.9 kcal/mol, respectively. The dashed lines present the same calculations but after removing the ions from the cavity and S4. The removal of the ion-ion repulsion decreases the free-energy difference between S1 and the bulk by about 4 kcal/mol, but the wells remain shallow.

(B) Around binding site S4, in the absence of an ion in S1, free-energy wells are found around $Z = -7$ Å and $Z = -6$ Å for K⁺ and Na⁺, respectively. The wells are shallow, at 1.5 kcal/mol for K⁺ and 2.4 kcal/mol for Na⁺. A metastable well is seen around $Z = -5$ Å (identified by an asterisk), corresponding to the upper position of K⁺ in S4, as illustrated in Figure 1. Adding an ion in the cavity would further stabilize this binding site because of the electrostatic repulsion between the two ions. The important free-energy barrier around $Z = \pm 3.5$ Å potentially prevents the permeation of K⁺ and Na⁺. The reference point is set to 0 kcal/mol at $Z = 13$ Å for PMFs shown in (A), and at $Z = -9.5$ Å for those shown in (B). Convergence of the PMF calculations is illustrated in Figure S4.

associated free-energy calculations are consistent with the data from the titration experiment and the experimental electronic density. Taken together, the experiments and the

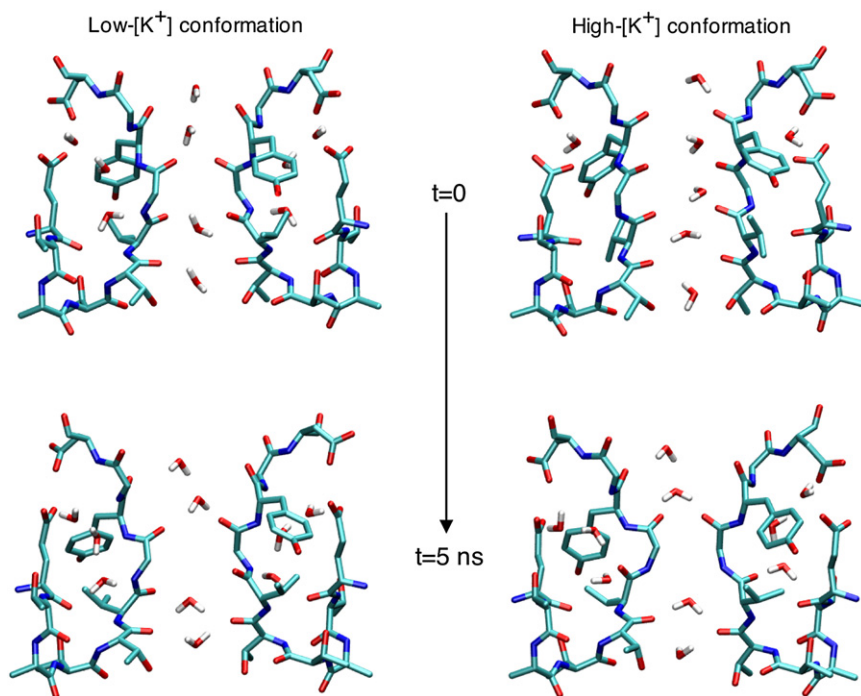


Figure 6. Conformation of the Selectivity Filter as Observed in Simulations of the Low-[K⁺] and Canonical High-[K⁺] Structures with All Bound Ions Replaced by Water Molecules

The low-[K⁺] structure remained stable throughout the simulation. After a few nanoseconds of simulation, the high-[K⁺] structure adopts a 4-fold symmetric conformation that is quite similar to the low-[K⁺] one. In both cases, four water molecules are found in the pore, and, in each of the four monomers, three water molecules in a cavity adjacent to the pore lumen closely interact with the selectivity filter. Only two of the four subunits are shown for the sake of clarity.

K⁺ channels can be depleted of ions at any stage of conduction and gating. The possibility that the inactivated state could be deprived of ions challenges the idea that the absence of K⁺ in the selectivity filter of K⁺ channels would lead them to adopt a defunct state—distinct from the inactivated one—from which recovery is slow or, in some cases, impossible (Loboda et al., 2001; Ambriz-Rivas et al., 2005). Different experiments performed

molecular mechanics calculations support the idea that the low-[K⁺] conformation has little ion-binding affinity. This conclusion should also apply to the latest structures obtained by Perozo and colleagues (Cuello et al., 2010) depicting a putative open-inactivated state of KcsA, in which the selectivity filter adopts a conformation that appears to be similar to the low-[K⁺] structure.

Proposed models of gating in the selectivity filter of KcsA generally involve transitions between conducting states containing two ions and nonconducting ones containing only one ion (Zhou et al., 2001; Lockless et al., 2007; Cuello et al., 2010). Although not contradicting such models, the description of dynamic features and energetics that we present here provides a different perspective. Our PMF calculations support the idea that the low-[K⁺] structure binds at most one ion as proposed in the X-ray analyses. Contrary to the canonical high-[K⁺] structure, the low-[K⁺] conformation actually opposes to the binding of a second ion by about 3 kcal/mol. However, our results also show that the selectivity filter has only little binding affinity for the first ion, suggesting an equilibrium between states with zero and one ion. Such equilibrium states would hardly be detectable by isothermal titration calorimetry (ITC) measurements, potentially explaining why only one K⁺ is seen binding to KcsA in the ITC experiments of Lockless et al. (2007).

Studies of different channels of the Kv family have led many authors to depict C-type inactivation as a collapse of the selectivity filter (Liu et al., 1996; Kiss and Korn, 1998). The low-[K⁺] structure, pinched at the level of the S2 binding site, provides support for such a model and has often been associated with a C-type inactivated state of K⁺ channels (Yellen, 2001; Cordero-Morales et al., 2007; Ader et al., 2008). In light of our findings, one should ask if the selectivity filter of KcsA and other

in absence of K⁺ suggest that KcsA can better sustain such conditions than its eukaryotic counterparts, supporting the idea that K⁺ is not absolutely essential to the stability of KcsA (Saparov and Pohl, 2004; Imai et al., 2010). Although there is no clear demonstration that the low-[K⁺] conformation is actually visited under normal conditions of permeation and gating, some structural studies support the idea that the low-[K⁺] structure, which according to our calculations would be depleted of ions, could correspond to the inactivated state of KcsA (Imai et al., 2010; Cuello et al., 2010).

Whether this ion-depleted low-[K⁺] structure could also correspond to the inactivated state of eukaryotic channels remains unclear. Besides the fact that ions seem to play an important role in the stability of these channels, functional studies, notably on Shaker and Kv1.3, suggest that at least one ion remains continuously bound to the filter. In Shaker the C-type inactivated state is permeable to Na⁺ when K⁺ is removed completely, but a low concentration of K⁺ is sufficient to block the Na⁺ current without producing any measurable K⁺ current (Starkus et al., 1997; Kiss and Korn, 1998). This suggests that the transition to the C-type inactivated state involves some conformational change of the selectivity filter that prevents the conduction of K⁺ but allows the binding of at least one K⁺ with high affinity (Yellen, 1998). Studies on the mechanism of recovery from inactivation also strongly suggest that at least one ion remains bound to the filter. In Kv1.3, recovery from inactivation was shown to be voltage dependent and influenced by the extracellular concentration of permeating and nonpermeating cations, such as tetraethylammonium (TEA). A plausible model proposed by Levy and Deutsch (1996a) suggests that an ion already bound to the filter moves to a key regulatory site under the influence of both the applied transmembrane potential and the electrostatic (or

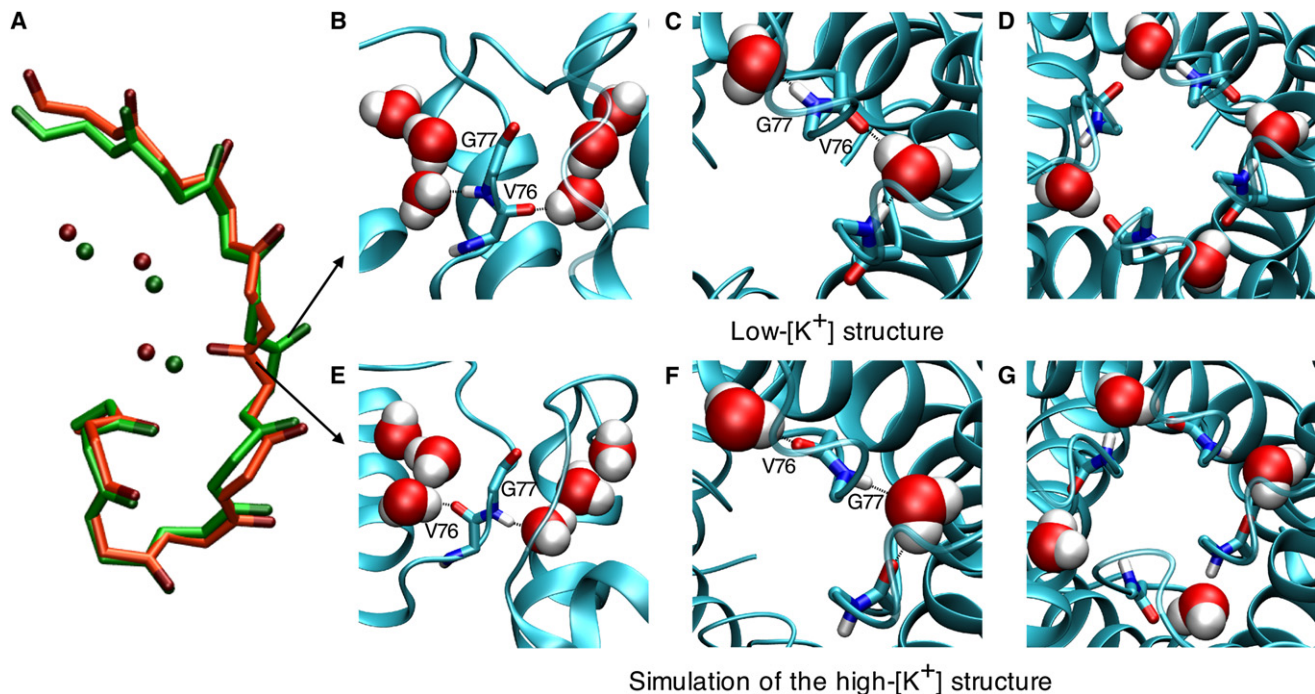


Figure 7. Two Configurations of the Selectivity Filter and the Surrounding Network of Hydrogen-Bonded Water Molecules

(A) The backbone of the selectivity filter obtained after simulation of the ion-free high-[K⁺] structure (orange), including the three water molecules found in its vicinity, superposes quite well with the experimental low-[K⁺] structure (green). However, the Val76/Gly77 amide plane is rotated by about 180°.

(B–G) The molecular representations highlight the interactions taking place between the backbone and surrounding water molecules for both possible conformations of the Val76/Gly77 amide plane.

(B and E) show side views of two adjacent subunits illustrating that the Val76/Gly77 amide planes make hydrogen bonds with the lowest of the surrounding water molecules.

(C, D, F, and G) show top views of the same interactions. For both orientations of the amide plane, a closed network of hydrogen bonds is formed, though it propagates in opposite directions (D and G). Further comparison of the different conformations of the selectivity filter is presented in Figures S5 and S6.

allosteric) repulsion from an externally bound ion. [Baukrowitz and Yellen \(1996\)](#) have also hypothesized the existence of a regulatory binding site within the selectivity filter of Shaker. They have proposed that the release of K⁺ from this control site, and subsequently from the channel, would lead the channel to inactivate. Although this is a plausible mechanism, it does not seem essential to suppose that the ion actually leaves the selectivity filter. A simple displacement of the ions within the selectivity filter (see [Bernèche and Roux, 2005](#)) could also support the functional data. Although there is no formal proof of the presence of bound K⁺ in the selectivity filter of inactivated channels, these observations are indicative of possible discrepancies between the inactivation mechanisms of KcsA and eukaryotic Kv channels.

A parallel between the inactivation of KcsA and the C-type inactivation of eukaryotic Kv channels was drawn on the basis that extracellular K⁺ concentration modulates the onset rate of both mechanisms ([Chakrapani et al., 2007](#)). However, to determine to what extent these mechanisms are related, further properties should be compared. Information on the actual C-type inactivated state of different K⁺ channels could in part be provided by comparative studies of the factors influencing recovery from inactivation ([Levy and Deutsch, 1996b](#); [Ray and Deutsch, 2006](#)), a mechanism that bears important physiological implications ([Rasmusson et al., 1995](#)). To be complete, models describing (C-type) inactivation of K⁺ channels should integrate

the permeation, inactivation, and recovery from inactivation processes, accounting for the eventual entry and exit of ions. Models of inactivation gating that were proposed on the basis of X-ray diffraction data involve that the exit of one ion leads the channel to inactivate, leaving one ion in the selectivity filter ([Zhou et al., 2001](#); [Lockless et al., 2007](#); [Cuello et al., 2010](#)). Our calculations suggest that in the case of KcsA, the remaining ion would be loosely bound and the filter practically filled with water molecules. The detailed mechanism of such an inactivation process remains unknown, and whether it would also apply to eukaryotic channels is unclear.

EXPERIMENTAL PROCEDURES

Molecular Systems

Two molecular membrane systems were built based on the KcsA channel in its high-[K⁺] (PDB entry 1K4C) and low-[K⁺] (PDB entry 1K4D) conformations ([Zhou et al., 2001](#)). In both cases, all residues were assigned their standard protonation state at pH 7, except Glu71, which was protonated. The systems were assembled using the CHARMM-GUI web service ([Jo et al., 2008](#)) following a protocol developed by [Woolf and Roux \(1994\)](#). The protein channel, with its symmetry axis aligned along the z axis, was embedded in a lipid bilayer of 156 dipalmitoylphosphatidylcholine (DPPC) molecules. The number of ions in the bulk was adjusted to reproduce experimental ionic concentrations (150 mM KCl for high-[K⁺], 150 mM NaCl for low-[K⁺]) and to obtain neutral systems, for a total of 24 cations and 36 anions. Each molecular system contained about 59,170 atoms.

All calculations were performed using the CHARMM software version c34 (Brooks et al., 1983). The all-atom potential energy function PARAM27 (Mackerell et al., 2004) was used for protein and phospholipids, and water molecules were modeled using the TIP3P potential (Jorgensen et al., 1983). The Lennard-Jones parameters for the cation-carbonyl oxygen pair interactions were refined to yield solvation free energies in liquid N-methylacetamide (NMA), similar to those in bulk water (Roux and Bernèche, 2002). Although the solvation free energy of K⁺ and Na⁺ in liquid NMA is not known experimentally, data from other liquid amides suggest that it should be within 1–2 kcal/mol of bulk water values (Cox et al., 1974). Periodic boundary conditions were applied, and long-range electrostatic interactions were treated by the particle mesh Ewald algorithm (Essmann et al., 1995). The molecular systems were equilibrated for about 300 ps with decreasing harmonic restraints applied to the protein atoms, the pore ions, and the water molecules localized in the P loop and the filter. All trajectories were generated with a time step of 2 fs at constant normal pressure (1 Atm) controlled by an extended Lagrangian algorithm (Feller et al., 1995) and constant temperature (323 K) using a Nosé-Hoover thermostat (Nosé, 1984; Hoover, 1985). Both systems were simulated with various starting ion occupancy states as listed in Table 1.

Calculation of Radial Distribution Functions

Radial distribution functions $g(r)$ were calculated by counting the number of coordinating atoms within concentric spherical shells with a thickness of 0.04 Å and a radius r , centered on the targeted ion. The functions were normalized by the volume of each shell. Integration of these functions provided the number of coordination ligands, $n(r)$, within a given distance, r . Conformation sampling is limited by the stability of ions in their binding site. Thus, the $g(r)$ and $n(r)$ functions were averaged over segments of 800 ps, specified in the relevant figure captions.

PMF Calculations

The PMF calculations were performed according to the umbrella sampling approach. The reaction coordinate was defined as the distance along the pore axis (which is aligned with the z axis) between the ion and the center of mass of the selectivity filter. Independent simulations of 1 ns were performed every 0.5 Å along this reaction coordinate using a biasing harmonic potential with a force constant of 20 kcal/mol·Å² and were unbiased using the weighted histogram analysis method (WHAM) (Kumar et al., 1992). The reference free-energy values were set to zero away from the selectivity filter. The convergence of the umbrella sampling simulations is illustrated in Figure S4.

SUPPLEMENTAL INFORMATION

Supplemental Information includes six figures and can be found with this article online at doi:10.1016/j.str.2010.10.008.

ACKNOWLEDGMENTS

We are grateful to C. Deutsch for helpful comments on a previous version of the manuscript. This work has been supported by a grant from the Swiss National Science Foundation to S. B. (SNF-Professorship No. 118928).

Received: May 10, 2010

Revised: October 14, 2010

Accepted: October 14, 2010

Published: January 11, 2011

REFERENCES

- Ader, C., Schneider, R., Hornig, S., Velisetty, P., Wilson, E.M., Lange, A., Giller, K., Ohmert, I., Martin-Eaucclair, M.F., Trauner, D., et al. (2008). A structural link between inactivation and block of a K⁺ channel. *Nat. Struct. Mol. Biol.* **15**, 605–612.
- Ambriz-Rivas, M., Islas, L.D., and Gomez-Lagunas, F. (2005). K⁺-dependent stability and ion conduction of Shab K⁺ channels: a comparison with Shaker channels. *Pflugers Arch.* **450**, 255–261.
- Baukowitz, T., and Yellen, G. (1996). Use-dependent blockers and exit rate of the last ion from the multi-ion pore of a K⁺ channel. *Science* **271**, 653–656.
- Bean, B.P. (2007). The action potential in mammalian central neurons. *Nat. Rev. Neurosci.* **8**, 451–465.
- Bernèche, S., and Roux, B. (2001). Energetics of ion conduction through the K⁺ channel. *Nature* **414**, 73–77.
- Bernèche, S., and Roux, B. (2005). A gate in the selectivity filter of potassium channels. *Structure* **13**, 591–600.
- Brooks, B.R., Brucoleri, R.E., Olafson, B.D., States, D.J., Swaminathan, S., and Karplus, M. (1983). CHARMM: a program for macromolecular energy, minimization, and dynamics calculations. *J. Comput. Chem.* **4**, 187–217.
- Chakrapani, S., Cordero-Morales, J.F., and Perozo, E. (2007). A quantitative description of KcsA gating I: macroscopic currents. *J. Gen. Physiol.* **130**, 465–478.
- Cordero-Morales, J.F., Cuello, L.G., Zhao, Y., Jogini, V., Cortes, D.M., Roux, B., and Perozo, E. (2006). Molecular determinants of gating at the potassium-channel selectivity filter. *Nat. Struct. Mol. Biol.* **13**, 311–318.
- Cordero-Morales, J.F., Jogini, V., Lewis, A., Vásquez, V., Cortes, D.M., Roux, B., and Perozo, E. (2007). Molecular driving forces determining potassium channel slow inactivation. *Nat. Struct. Mol. Biol.* **14**, 1062–1069.
- Cox, B.G., Hedwig, G.R., Parker, A.J., and Watts, D.W. (1974). Solvation of ions. XIX Thermodynamic properties for transfer of single ions between protic and dipolar aprotic solvents. *Aust. J. Chem.* **27**, 477–501.
- Cuello, L.G., Jogini, V., Cortes, D.M., and Perozo, E. (2010). Structural mechanism of C-type inactivation in K(+) channels. *Nature* **466**, 203–208.
- Domene, C., and Furini, S. (2009). Dynamics, energetics, and selectivity of the low-K⁺ KcsA channel structure. *J. Mol. Biol.* **389**, 637–645.
- Domene, C., Klein, M.L., Branduardi, D., Gervasio, F.L., and Parrinello, M. (2008). Conformational changes and gating at the selectivity filter of potassium channels. *J. Am. Chem. Soc.* **130**, 9474–9480.
- Essmann, U., Perera, L., Berkowitz, M.L., Darden, T., Lee, H., and Pedersen, L.G. (1995). A smooth particle mesh Ewald method. *J. Chem. Phys.* **103**, 8577–8593.
- Feller, S.E., Zhang, Y.H., Pastor, R.W., and Brooks, B.R. (1995). Constant-pressure molecular-dynamics simulation: the Langevin piston method. *J. Chem. Phys.* **103**, 4613–4621.
- Furini, S., Beckstein, O., and Domene, C. (2009). Permeation of water through the KcsA K⁺ channel. *Proteins* **74**, 437–448.
- Gao, L., Mi, X., Paajanen, V., Wang, K., and Fan, Z. (2005). Activation-coupled inactivation in the bacterial potassium channel KcsA. *Proc. Natl. Acad. Sci. USA* **102**, 17630–17635.
- Hoover, W.G. (1985). Canonical dynamics: equilibrium phase-space distributions. *Phys. Rev. A* **31**, 1695–1697.
- Imai, S., Osawa, M., Takeuchi, K., and Shimada, I. (2010). Structural basis underlying the dual gate properties of KcsA. *Proc. Natl. Acad. Sci. USA* **107**, 6216–6221.
- Jo, S., Kim, T., Iyer, V.G., and Im, W. (2008). CHARMM-GUI: a web-based graphical user interface for CHARMM. *J. Comput. Chem.* **29**, 1859–1865.
- Jorgensen, W.L., Chandrasekhar, J., Madura, J.D., Impey, R.W., and Klein, M.L. (1983). Comparison of simple potential functions for simulating liquid water. *J. Chem. Phys.* **79**, 926–935.
- Kiss, L., and Korn, S.J. (1998). Modulation of C-type inactivation by K⁺ at the potassium channel selectivity filter. *Biophys. J.* **74**, 1840–1849.
- Kumar, S., Bouzida, D., Swendsen, R.H., Kollman, P.A., and Rosenberg, J.M. (1992). The weighted histogram analysis method for free-energy calculations on biomolecules. 1. The method. *J. Comput. Chem.* **13**, 1011–1021.
- Lenaeus, M.J., Vamvouka, M., Focia, P.J., and Gross, A. (2005). Structural basis of TEA blockade in a model potassium channel. *Nat. Struct. Mol. Biol.* **12**, 454–459.
- Levy, D.I., and Deutsch, C. (1996a). A voltage-dependent role for K⁺ in recovery from C-type inactivation. *Biophys. J.* **71**, 3157–3166.
- Levy, D.I., and Deutsch, C. (1996b). Recovery from C-type inactivation is modulated by extracellular potassium. *Biophys. J.* **70**, 798–805.

- Liu, Y., Jurman, M.E., and Yellen, G. (1996). Dynamic rearrangement of the outer mouth of a K⁺ channel during gating. *Neuron* 16, 859–867.
- Loboda, A., Melishchuk, A., and Armstrong, C. (2001). Dilated and defunct K channels in the absence of K⁺. *Biophys. J.* 80, 2704–2714.
- Lockless, S.W., Zhou, M., and Mackinnon, R. (2007). Structural and thermodynamic properties of selective ion binding in a K(+) channel. *PLoS Biol.* 5, e121.
- Mackerell, A.D., Feig, M., and Brooks, C.L. (2004). Extending the treatment of backbone energetics in protein force fields: limitations of gas-phase quantum mechanics in reproducing protein conformational distributions in molecular dynamics simulations. *J. Comput. Chem.* 25, 1400–1415.
- Nosé, S. (1984). A unified formulation of the constant temperature molecular-dynamics methods. *J. Chem. Phys.* 81, 511–519.
- Rasmusson, R.L., Morales, M.J., Castellino, R.C., Zhang, Y., Campbell, D.L., and Strauss, H.C. (1995). C-type inactivation controls recovery in a fast inactivating cardiac K⁺ channel (Kv1.4) expressed in *Xenopus* oocytes. *J. Physiol.* 489, 709–721.
- Ray, E.C., and Deutsch, C. (2006). A trapped intracellular cation MODULATES K⁺ channel recovery from slow inactivation. *J. Gen. Physiol.* 128, 203–217.
- Roux, B., and Bernèche, S. (2002). On the potential functions used in molecular dynamics simulations of ion channels. *Biophys. J.* 82, 1681–1684.
- Saparov, S.M., and Pohl, P. (2004). Beyond the diffusion limit: water flow through the empty bacterial potassium channel. *Proc. Natl. Acad. Sci. USA* 101, 4805–4809.
- Smith, P.L., Baukrowitz, T., and Yellen, G. (1996). The inward rectification mechanism of the HERG cardiac potassium channel. *Nature* 379, 833–836.
- Starkus, J.G., Kuschel, L., Rayner, M.D., and Heinemann, S.H. (1997). Ion conduction through C-type inactivated Shaker channels. *J. Gen. Physiol.* 110, 539–550.
- Woolf, T.B., and Roux, B. (1994). Molecular dynamics simulation of the gramicidin channel in a phospholipid bilayer. *Proc. Natl. Acad. Sci. USA* 91, 11631–11635.
- Yellen, G. (1998). The moving parts of voltage-gated ion channels. *Q. Rev. Biophys.* 31, 239–295.
- Yellen, G. (2001). Keeping K⁺ completely comfortable. *Nat. Struct. Biol.* 8, 1011–1013.
- Zhou, Y., and MacKinnon, R. (2003). The occupancy of ions in the K⁺ selectivity filter: charge balance and coupling of ion binding to a protein conformational change underlie high conduction rates. *J. Mol. Biol.* 333, 965–975.
- Zhou, Y., Morais-Cabral, J.H., Kaufman, A., and MacKinnon, R. (2001). Chemistry of ion coordination and hydration revealed by a K⁺ channel-Fab complex at 2.0 Å resolution. *Nature* 414, 43–48.